Contribution from the Department of Chemistry,
University of California, Santa Barbara, California 93106

Preparation and Spectral and Electrochemical Characterization of Dirhodium(II) Complexes with Bridging 1,8-Naphthyridine Ligands: 2,7-Bis(2-pyridyl)-1,8-naphthyridine, 5,6-Dihydrodipyrido[2,3-*b*:3′,2′-*j*][1,10]phenanthroline, 2-(2-Pyridyl)-1,8-naphthyridine, and 1,8-Naphthyridine. X-ray Crystal Structure of Tris(μ-acetato)(2,7-bis(2-pyridyl)-1,8-naphthyridine)dirhodium(II) Hexafluorophosphate

WAYNE R. TIKKANEN, E. BINAMIRA-SORIAGA, WILLIAM C. KASKA,* and PETER C. FORD*

Received April 12, 1983

The preparations and spectral and electrochemical characterizations of several dirhodium(II) complexes of substituted 1,8-naphthyridines are described. These dinuclear complexes are derived by reaction of the appropriate polydentate 1,8-naphthyridine species with dirhodium tetraacetate. The monosubstituted derivatives $Rh_2(O_2CCH_3)_3L^+$ include complexes of the crescent-shaped ligand 2,7-bis(2-pyridyl)-1,8-naphthyridine (bpnp) and of 5,6-dihydrodipyrido[2,3-*b*:3′,2′-*j*]-[1,10]phenanthroline (dinp) and 2-(2-pyridyl)-1,8-naphthyridine (pynp). A disubstituted complex, $Rh_2(O_2CCH_3)_2(pynp)_2^{2+}$, and a tetrasubstituted derivative, $[Rh_2(np)_4]Cl_4$ (np = 1,8-naphthyridine), are also described. Each of these compounds displays electronic spectral bands in the visible region that have been assigned as metal to ligand charge-transfer absorptions not seen in the parent tetraacetate. The electrochemical properties as studied by cyclic voltammetry also differ significantly from those of the tetraacetate with the mono- and disubstituted derivatives displaying both reversible oxidations *and* reductions. The spectral properties of these complexes are discussed in terms of their probable structures. The structure of the bpnp adduct, $[Rh_2(O_2CCH_3)_3bpnp]PF_6$, has been determined by X-ray diffraction techniques and refined by full-matrix least-squares procedures to a final *R* index of 0.068. Crystals are tetragonal, space group $I4_1cd$, with cell dimensions $a = b = 28.720$ (14) Å, $c = 13.906$ (5) Å, and $V = 11\,470$ (9) Å^3 and with $Z = 16$. The two rhodium atoms are bridged by three acetate groups and the naphthyridine fragment of bpnp. The 2-pyridyl nitrogen atoms occupy the axial sites trans to the Rh–Rh bond (Rh–Rh distance = 2.405 (2) Å).

Introduction

Bis ligand adducts of tetrakis(μ-carboxylato)dirhodium(II), $Rh_2(RCO_2)_4L_2$, have been extensively studied; recently, two comprehensive reviews of these complexes have been published.[1] There have been relatively few studies of complexes with a single bridging carboxylate substituted by either chelating or bridging ligands and none where one bridging acetate has been replaced by a neutral bridging ligand until a recent preliminary report from these laboratories.[2] This report was of a new complex, $Rh_2(O_2CCH_3)_3(bpnp)^+$, where the tetradentate ligand 2,7-bis(2-pyridyl)-1,8-naphthyridine (bpnp) occupies the coordination sites of the axial ligands, L, and of an acetate group. The combination of the crescent-shaped ligand bpnp and the dirhodium(II) center forms a "croissant complex" that displays physical and electrochemical properties unlike those of the dirhodium(II) tetracarboxylates. These properties are described in greater detail here. In addition, this paper details the synthesis and the physical and electrochemical properties for two other monosubstituted dirhodium(II) acetate complexes, $Rh_2(O_2CCH_3)_3L^+$ (L = 2-(2-pyridyl)-1,8-naphthyridine (pynp) and 5,6-dihydrodipyrido[2,3-*b*:3′,2′-*j*][1,10]phenanthroline (dinp), for a disubstituted complex, $Rh_2(O_2CCH_3)_2L_2^{2+}$ (L = pynp), and for the completely substituted tetrakis(1,8-naphthyridine)dirhodium(II) chloride. The structures of these ligands are shown in Figure 1.

Experimental Section

Solvents and Chemicals. Solvents were Mallinckrodt AR or SpectrAR quality. When higher purity was desired, the following procedures were used. Acetone was distilled from barium oxide under argon. Methylene chloride was distilled from lithium aluminum hydride under argon. Acetonitrile was distilled from calcium hydride under argon; the first fraction was discarded. Dimethylformamide (DMF) was vacuum distilled prior to use. Tetra-*n*-butylammonium perchlorate (TBAP) from Aldrich was recrystallized from ethyl acetate and stored under vacuum over phosphorus pentoxide.

Dirhodium(II) tetraacetate was used as received from Strem Chemicals. The 1,8-naphthyridine was prepared by the method of Paudler and Kress.[3] The bpnp, dinp, and pynp ligands were prepared as described by Caluwe.[4,5] Manipulation of air-sensitive compounds was accomplished by standard Schlenk techniques or in a Vacuum Atmospheres Corporation drybox with an argon atmosphere. Elemental analyses were performed by either the Alfred Bernhardt Mikroanalytisches Laboratorium of Engelskirchen, West Germany, or Schwarzkopf Microanalytical Laboratories of Woodside, NY.

Electrochemistry. Cyclic voltammetry was performed with a Chemtrix SSP-1 unit modified in house to the specifications of the SSP-2 three-electrode system. A three-compartment cell was used with a platinum wire auxiliary electrode and a saturated sodium chloride calomel (SSCE) reference electrode. The working electrode was either a platinum ball or planar pyrolytic graphite that was cleaned prior to each run. Reversibility of the waves was determined by comparison of the separation of anodic and cathodic peak potentials to that for internal ferrocene and by the ratio of anodic to cathodic peak currents (unity for a reversible process).

Physical Measurements. UV–visible and near-infrared data were obtained with Cary 14 and 118 spectrophotometers. Infrared spectra were obtained on Perkin-Elmer 283 and 683 spectrometers and calibrated with polystyrene. Samples were usually in KBr pellets or, when halide exchange was a possibility, as Nujol mulls between CsI plates.

Conductivity measurements were obtained with a Radiometer CDM2e conductivity meter in spectral grade nitromethane or triply distilled water. NMR spectra were recorded on Varian CFT-20 and XL-100 spectrometers. The 300-MHz NMR spectra were measured with a Nicolet NT-300 spectrometer. The 500-MHz spectra were obtained from the NSF Regional NMR Facility at the California Institute of Technology.

X-ray Crystallographic Analysis of $[Rh_2(O_2CCH_3)_3bpnp]PF_6$ (I). A crystal of approximate dimensions 0.18 × 0.28 × 0.15 mm was

(1) (a) Walton, R. A.; Cotton, F. A. "Multiple Bonds between Metal Atoms"; Wiley: New York, 1982; Chapter 7. (b) Felthouse, T. R. *Prog. Inorg. Chem.* **1982**, *29*, 74–166.
(2) Tikkanen, W. R.; Binamira-Soriaga, E.; Kaska, W. C.; Ford, P. C. *Inorg. Chem.* **1983**, *22*, 1147.
(3) Paudler, E. E.; Kress, T. J. *J. Org. Chem.* **1967**, *32*, 832.
(4) Caluwe, P. *Macromolecules* **1979**, *12*, 803.
(5) Majewicz, T. G.; Caluwe, P. *J. Org. Chem.* **1979**, *44*, 531–535.

0020-1669/84/1323-0141$01.50/0

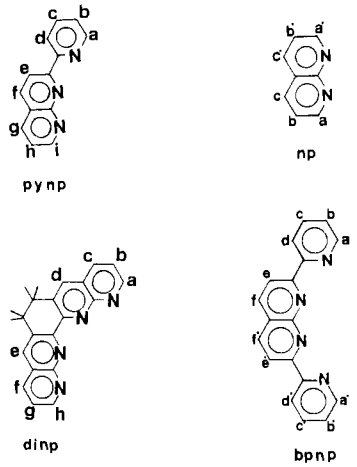

Figure 1. Structures of ligands used in this study with proton positions labeled.

Table I. Positional Parameters for the Non-Hydrogen Atoms of $[Rh_2(O_2CCH_3)_3bpnp]PF_6$[a,b]

atom	x	y	z
Rh(1)	0.1093 (0)	0.0973 (0)	0.3183 (0)
Rh(2)	0.1745 (0)	0.0450 (0)	0.3073 (2)
N(1)	0.0614 (5)	0.1570 (5)	0.3188 (15)
N(2)	0.1543 (5)	0.1498 (5)	0.3065 (12)
N(3)	0.2174 (5)	0.1005 (5)	0.3065 (14)
N(4)	0.2427 (5)	0.0108 (5)	0.3085 (17)
O(1)	0.1196 (6)	0.0975 (5)	0.4686 (12)
O(2)	0.1778 (5)	0.0449 (5)	0.4575 (13)
O(3)	0.1035 (4)	0.0932 (4)	0.1757 (10)
O(4)	0.1667 (5)	0.0475 (4)	0.1642 (10)
O(5)	0.0669 (4)	0.0391 (4)	0.3317 (10)
O(6)	0.1284 (4)	−0.0086 (4)	0.3114 (13)
C(1)	0.1505 (7)	0.0726 (7)	0.5056 (15)
C(2)	0.1579 (8)	0.0744 (8)	0.6130 (17)
C(3)	0.1333 (8)	0.0676 (7)	0.1289 (16)
C(4)	0.1259 (9)	0.0646 (9)	0.0216 (18)
C(5)	0.0854 (5)	−0.0003 (8)	0.3228 (19)
C(6)	0.0521 (7)	−0.0424 (7)	0.3185 (19)
C(7)	0.0142 (6)	0.1583 (6)	0.3285 (16)
C(8)	−0.0113 (6)	0.1978 (6)	0.3202 (18)
C(9)	0.0128 (6)	0.2406 (7)	0.3069 (20)
C(10)	0.0622 (7)	0.2392 (7)	0.2975 (16)
C(11)	0.0841 (6)	0.1978 (6)	0.3069 (16)
C(12)	0.1358 (6)	0.1934 (6)	0.2991 (16)
C(13)	0.1661 (6)	0.2331 (6)	0.2902 (13)
C(14)	0.2118 (7)	0.2282 (7)	0.2882 (15)
C(15)	0.2325 (7)	0.1835 (7)	0.2964 (16)
C(16)	0.2010 (6)	0.1451 (6)	0.3034 (16)
C(17)	0.2810 (7)	0.1736 (7)	0.2903 (15)
C(18)	0.2942 (6)	0.1286 (6)	0.2951 (14)
C(19)	0.2635 (6)	0.0929 (6)	0.3032 (15)
C(20)	0.2791 (6)	0.0424 (6)	0.3042 (18)
C(21)	0.3241 (7)	0.0278 (7)	0.3149 (19)
C(22)	0.3342 (8)	−0.0202 (8)	0.3228 (19)
C(23)	0.2988 (7)	−0.0518 (8)	0.3190 (22)
C(24)	0.2537 (7)	−0.0346 (7)	0.3096 (20)
P(1)	−0.1578	0.1813	0.3459
F(1)	−0.1864	0.1368	0.3600
F(2)	−0.2018	0.2106	0.3601
F(3)	−0.1292	0.2257	0.3319
F(4)	−0.1139	0.1520	0.3316
F(5)	−0.1673	0.1794	0.2377
F(6)	−0.1483	0.1831	0.4541

[a] Atoms are labeled as shown in Figure 2. [b] The estimated standard deviations of the least significant digits are given in parentheses.

mounted and aligned on a Syntex P$\bar{1}$ automated diffractometer with graphite-monochromatized Mo Kα radiation (λ = 0.7107 Å). A low-temperature attachment maintained the crystal temperature at 115 K. The tetragonal cell parameters, as determined by a least-squares treatment of the angular coordinates of 15 independent reflections with 2θ values up to 26°, are $a = b = 28.720$ (14) Å, $c = 13.906$ (5) Å, and $V = 11\,470$ (9) Å^3. Axial photographs confirmed the chosen cell and the *mmm* Laue symmetry. For 16 molecules of I per unit cell, the calculated density is 1.881 g/cm^3; the density measured by flotation in *m*-xylene/methyl iodide solution is 1.879 g/cm^3. The intensity data were measured by using a θ–2θ scan mode with a scan speed of 6°/min. The intensities of 3 check reflections monitored every 100 reflections showed no significant variations. Of the 5725 reflections measured (with $2\theta \leq 50°$), 2144 independent reflections had $I > 3\sigma(I)$ and only these were used in subsequent calculations. The intensities were corrected for Lorentz and polarization effects and for the absorption of X rays (μ = 12.66 cm^{-1}). The computer programs employed have been described previously.[6]

Table II. Selected Bond Lengths (Å) and Bond Angles (deg) for $[Rh_2(O_2CCH_3)_3bpnp]PF_6$[a]

Rh(1)-Rh(2)	2.405 (2)	C(3)-O(4)	1.22 (2)
Rh(1)-N(1)	2.202 (15)	C(5)-O(5)	1.26 (2)
Rh(1)-N(2)	1.992 (13)	C(5)-O(6)	1.27 (2)
Rh(2)-N(3)	2.015 (14)	N(1)-C(7)	1.36 (2)
Rh(2)-N(4)	2.189 (16)	N(1)-C(11)	1.35 (2)
Rh(1)-O(1)	2.112 (17)	N(2)-C(12)	1.36 (2)
Rh(1)-O(3)	1.993 (14)	N(2)-C(16)	1.35 (2)
Rh(1)-O(5)	2.076 (13)	N(3)-C(16)	1.36 (2)
Rh(2)-O(2)	2.091 (18)	N(3)-C(19)	1.34 (2)
Rh(2)-O(4)	2.004 (14)	N(4)-C(20)	1.39 (2)
Rh(2)-O(6)	2.030 (12)	N(4)-C(24)	1.34 (2)
C(1)-O(1)	1.25 (2)	C(1)-C(2)	1.51 (3)
C(1)-O(2)	1.30 (2)	C(3)-C(4)	1.51 (3)
C(3)-O(3)	1.30 (2)	C(5)-C(6)	1.54 (3)
Rh(2)-Rh(1)-N(1)	167.1 (4)	Rh(1)-Rh(2)-N(3)	88.9 (4)
Rh(2)-Rh(1)-N(2)	87.9 (4)	Rh(1)-Rh(2)-N(4)	167.2 (4)
Rh(2)-Rh(1)-O(1)	87.5 (4)	Rh(1)-Rh(2)-O(2)	88.4 (4)
Rh(2)-Rh(1)-O(3)	88.1 (4)	Rh(1)-Rh(2)-O(4)	87.3 (4)
Rh(2)-Rh(1)-O(5)	87.7 (3)	Rh(1)-Rh(2)-O(6)	87.9 (3)
N(1)-Rh(1)-N(2)	79.3 (5)	N(3)-Rh(2)-N(4)	79.0 (6)
N(1)-Rh(1)-O(1)	94.7 (7)	N(3)-Rh(2)-O(2)	88.8 (7)
N(1)-Rh(1)-O(3)	89.8 (6)	N(3)-Rh(2)-O(4)	91.9 (6)
N(1)-Rh(1)-O(5)	105.1 (5)	N(3)-Rh(2)-O(6)	176.7 (5)
N(2)-Rh(1)-O(1)	89.4 (6)	O(2)-Rh(2)-O(4)	175.7 (6)
N(2)-Rh(1)-O(3)	90.9 (6)	O(2)-Rh(2)-O(6)	90.1 (7)
N(2)-Rh(1)-O(5)	175.6 (5)	O(4)-Rh(2)-O(6)	89.0 (6)
O(1)-Rh(1)-O(3)	175.5 (5)	N(4)-Rh(2)-O(2)	87.2 (7)
O(1)-Rh(1)-O(5)	89.7 (6)	N(4)-Rh(2)-O(4)	97.1 (7)
O(3)-Rh(1)-O(5)	89.6 (5)	N(4)-Rh(2)-O(6)	104.1 (5)

[a] The estimated standard deviations of the least significant digits are given in parentheses.

The systematic absences *hkl* ($h + k + l = 2n + 1$), 0*kl* ($l = 2n + 1$), and *hhl* ($2h + l = 4n + 1$) indicated the space group $I4_1cd$ (No. 110). *E*-value statistics suggested a noncentrosymmetric structure. The positional coordinates of the two Rh atoms were obtained by direct methods with MULTAN.[6] The remaining non-hydrogen atoms in the asymmetric unit were located by successive difference Fourier syntheses. The hexafluorophosphate ion was severely disordered; only one orientation of the anion was resolved, and this model was refined as a rigid group with a P–F distance of 1.53 Å.[7] The positions of the ring hydrogen atoms were calculated assuming idealized geometries; these atoms were assigned an isotropic thermal parameter equal to that of the carbon to which it was bonded. No attempt was made to locate the acetate hydrogens. All non-hydrogen atoms were refined isotropically except for the two Rh atoms, for which anisotropic temperature factors were varied. Neutral-atom scattering factors were used, and corrections for anomalous dispersion were applied.[8] Full-matrix least-squares refinement of 167 parameters led to convergence with $R = 0.068$ and $R_w = 0.086$, where $R = \sum||F_o| - |F_c||/\sum F_o$ and $R_w = [\sum w(F_o - |F_c|)^2/\sum wF_o^2]^{1/2}$. The largest peak in the final difference map, 2.0 e/Å^3, is in the vicinity of the PF_6^- ion and is due to the inadequacy of the model to account for the electron density

(6) Nemeh, S.; Jensen, C.; Binamira-Soriaga, E.; Kaska, W. C. *Organometallics* **1983**, *2*, 1442.
(7) Ondik, H.; Smith, D. "International Tables for X-ray Crystallography"; Kynoch Press: Birmingham, England, 1974; Vol. III, p 266.
(8) Cromer, D. T.; Waber, J. T. "International Tables for X-ray Crystallography"; Kynoch Press: Birmingham, England, 1974; Vol. IV, Tables 2.2A and 2.3.1.

Table III. Elemental Analyses of Dirhodium(II) Complexes of 1,8-Naphthyridines

compd	anal. calcd (found)		
	% C	% H	% N
$[Rh_2(OAc)_3(bpnp)]PF_6 \cdot 2H_2O$ (I)	35.49 (35.10)	2.60 (2.61)	6.90 (6.82)
$[Rh_2(OAc)_3(dinp)]PF_6 \cdot 3H_2O$ (II)	33.27 (33.11)		6.47 (6.47)
$[Rh_2(OAc)_3(pynp)]PF_6$ (III)	31.04 (30.86)		5.72 (5.69)
$[Rh_2(OAc)_2(pynp)_2](PF_6)_2$ (IV)	35.04 (35.02)		8.17 (8.34)
$Rh_2(np)_4Cl_4 \cdot 4H_2O$ (V)[a]	39.49 (39.37)		11.42 (11.48)

[a] % Cl: calcd, 14.52; found, 14.47.

in that region. Non-hydrogen atom coordinates for I are tabulated in Table I. Important interatomic distances and angles are given in Table II. Tables of hydrogen atom coordinates, anisotropic and isotropic thermal parameters for all atoms, bond distances and angles involving the bpnp ligand, least-squares planes, and observed and calculated structure factors are deposited as supplementary material.

Tris(μ-acetato)(2,7-bis(2-pyridyl)-1,8-naphthyridine)dirhodium(II) Hexafluorophosphate (I). To a magnetically stirred deaerated methanolic suspension of bpnp (30 mg, 105 μmol) and dirhodium(II) tetraacetate (47 mg, 105 μmol) under argon was added 1 equiv of acid (aqueous 1 M HCl). The initially pale blue solution immediately turned deep purple, and the solid ligand and rhodium acetate dissolved to give an intensely purple solution. The air-stable solution was then added to an aqueous solution of ammonium hexafluorophosphate and the methanol boiled off on a hot plate to turbidity. The solution was placed in a refrigerator overnight. The resulting fine purple needles were collected by filtration on a paper frit; yield 75 mg (88%). Crystals suitable for X-ray analysis were grown slowly from an acetonitrile/water solution. The infrared spectrum as a KBr disk shows the following absorptions: 3090 (br, w), 2910 (br, w), 1590 (s), 1568 (s), 1461 (7), 1432 (s), 1349 (w), 1310 (w), 1261 (2), 1151 (w), 1010 (w), 840 (s), 775 (s), 779 (m), 553 (s), 380 (w), 330 (w) cm^{-1}.

Tris(μ-acetato)(5,6-dihydrodipyrido[2,3-*b*:3′,2′-*j*][1,10]-phenanthroline)dirhodium(II) Hexafluorophosphate (II). To 20 mL of a deaerated methanol suspension of dinp (40 mg, 140 μmol) and dirhodium tetraacetate (70 mg, 160 μmol) under an argon atmosphere was added aqueous HCl (0.14 mL, 140 μmol) by syringe. The mixture was refluxed for 2 h to give a red-brown solution and then cooled overnight. Neutralization of the excess acid was carried out in air with solid sodium carbonate. The solution was gravity filtered and placed on a 1.2-m Sephadex LH-20 column. Elution with methanol gave first a small brown band, which was discarded. The second band, pink-orange, and the third band, purple, were saved. A green band, presumed to be rhodium acetate, and a following yellow band were both discarded. Addition of aqueous ammonium hexafluorophosphate to the purple fraction, boiling to turbidity, and cooling overnight at 5 °C gave 41 mg (33% based on dinp) of purple needles, soluble in common polar organic solvents.

Tris(μ-acetato)(2-(2-pyridyl)-1,8-naphthyridine)dirhodium(II) Hexafluorophosphate (III). To a stirred suspension of dirhodium tetraacetate (85 mg, 190 μmol) and pynp (30 mg, 145 μmol) in 20 mL of deaerated methanol under argon was added 0.15 mL of 1 M aqueous HCl by syringe. The mixture was refluxed for 10 h and then opened to air after cooling. Neutralization of excess acid with solid sodium carbonate was followed by gravity filtration. The clear red-brown filtrate solution was introduced to a 1.2-m column of Sephadex LH-20 and eluted with methanol. A golden brown band separated first, followed by a purple band, and then the green band of rhodium acetate starting material. The purple band was worked up by precipitating as the hexafluorophosphate salt as in the dinp complexes, and a yield of 17 mg (16% based on pynp) of red powder mixed with red crystals was obtained. The product was slightly soluble in water and very soluble in polar organic solvents, including acetone, methanol, and acetonitrile. The infrared spectrum of this material as a KBr disk shows the following absorptions: 3080 (br, w), 2950 (br, w), 1603 (m), 1570 (s), 1525 (w), 430 (br, s), 1355 (m), 1318 (w), 1266 (w), 1245 (w), 1210 (vw), 1148 (w), 1048 (w), 1018 (w), 840 (br, s), 778 (s), 748 (m), 718 (m), 638 (w), 556 (s), 370 (w) cm^{-1}.

Bis(μ-acetato)bis(2-(2-pyridyl)-1,8-naphthyridine)dirhodium(II) Hexafluorophosphate (IV). The golden brown fraction from the synthesis of III was worked up by precipitation of the complex ion as in that procedure. Collection by suction filtration gave 38 mg (25% based on pynp) of a golden brown powder. This material dissolves in water and polar organic solvents. Crystals were obtained by slow evaporation of aqueous acetonitrile solutions. The infrared spectrum obtained from a KBr pellet shows the following absorptions: 3090 (br, w), 2900 (br, w), 1610 (s), 1558 (m), 1528 (m), 1475 (m), 1438 (s, br), 1358 (m), 1318 (w), 1267 (w), 1245 (w), 1210 (w), 1176 (w), 1150 (m), 1080 (w), 1048 (w), 1016 (m), 840 (br, s), 778 (s), 748 (m), 718 (m), 638 (w), 556 (s), 370 (m) cm^{-1}.

Tetrakis(μ-1,8-naphthyridine)dirhodium(II) Tetrachloride Hexahydrate (V). To a stirred suspension of dirhodium tetraacetate (50 mg, 114 μmol) and 1,8-naphthyridine (60 mg, 470 μmol) in deaerated methanol under argon was added 0.5 mL of aqueous 1 M HCl by syringe. After 2 days of stirring at room temperature a yellow brown solution was obtained with some green solid. The mixture was brought to reflux for 1 h and then was left to cool to room temperature. Suction filtration separated the green solid and some red-brown crystalline material from the red-brown filtrate solution. An infrared spectrum of this green material shows acetate bands at 1600 and 1420 cm^{-1}. The filtrate solution was rotary evaporated to dryness and the resulting solid recrystallized from absolute ethanol and toluene to give a 35-mg yield of a reddish solid (35% based on Rh). The IR spectrum (KBr pellet) showed no absorptions in the asymmetric O–C–O (1600 cm^{-1}) or symmetric O–C–O (1420 cm^{-1}) stretching regions, confirming total substitution of the acetates. The product is soluble in water, methanol, and ethanol but is much less soluble in less polar solvents. Recrystallization from ethanol/butanol gave red-orange needles. The infrared spectrum of this compound as a KBr pellet shows the following absorptions: 3080 (m), 1610 (s), 1576 (m), 1516 (s), 1467 (w), 1434 (w), 1388 (m), 1348 (m), 1303 (m), 1264 (w), 1246 (w), 1209 (m), 1148 (m), 1078 (m), 838 (s), 788 (s), 668 (w), 538 (w), 500 (w), 466 (w), 438 (w), 307 (w) cm^{-1}.

Results and Discussion

The replacement of bridging acetate ligands on $Rh_2(CH_3CO_2)_4$ by 1,8-naphthyridine derivatives was accomplished with the addition of equimolar acid (e.g., eq 1 and 2). The elemental analyses for the resulting products are listed in Table III.

$$L + Rh_2(OAc)_4 + HX \rightarrow Rh_2(OAc)_3L^+ + X^- + HOAc \quad (1)$$

L = bpnp (I), dinp (II), pynp (III); $OAc^- = CH_3CO_2^-$

$$4L + Rh_2(OAc)_4 + 4HX \rightarrow Rh_2L_4X_4 + 4HOAc \quad (2)$$

L = 1,8-naphthyridine (V)

One of these complexes, tris(μ-acetato)(2,7-bis(2-pyridyl)-1,8-naphthyridine)dirhodium(II) hexafluorophosphate (I, see Figure 2), has been characterized by a single-crystal X-ray study described in a preliminary communication.[2] A comparison of this structure's key bond angles and bond lengths (Table II) with those of the tetraacetate analogue $Rh_2(OAc)_4(py)_2$[9] (VI) shows that the presence of the bpnp ligand in place of one bridging acetate and the two axial pyridines of VI has at most a modest effect upon the bonding in the remaining tris(μ-acetato)dirhodium(II) fragment. For example, the Rh–Rh bond distance in I is 2.405 (2) Å, only slightly longer than the 2.396-Å value found for VI, and the Rh–O lengths and O–Rh–O angles are essentially equivalent (within experimental uncertainties) for the two compexes. A key feature of I is that the bpnp ligand assumes a symmetrical

(9) Koh, Y. B.; Christoph, G. G. *Inorg. Chem.* **1978**, *17*, 2590.

Table IV. ^{1}H NMR Resonances in the Aromatic Region (from 500-MHz Spectrum) for I in Me_2SO-d_6 at 25 °C

H	chem shift, δ	coupling constant, Hz
a, a′	9.79	$J_{ab} = 4.3$
b, b′	8.33	$J_{ab} = 4.3, J_{bc} = 7.9$
c, c′	8.63	$J_{bc} = J_{cd} = 7.9, J_{ac} = 1.8$
d, d′	9.155	$J_{cd} = 7.9$
e, e′	9.145	$J_{ef} = 8.5$
f, f′	8.96	$J_{ef} = 8.5$

Table V. Upfield Region of ^{1}H NMR Spectra of the Dirhodium(II) μ-Acetato Complexes in Me_2SO-d_6

complex	chem shift, δ	ratio of integrals
$Rh_2(OAc)_4$	2.12	
$[Rh_2(OAc)_3(bpnp)][PF_6]$ (I)	1.36	2
	2.23	1
$[Rh_2(OAc)_3(dinp)][PF_6]$ (II)	1.49	2
	2.21	1
$[Rh_2(OAc)_3(pynp)][PF_6]$ (III)	1.50	1.9
	2.15	1.0
$[Rh_2(OAc)_2(pynp)_2][PF_6]_2$ (IV)	1.76	

bridging mode and is nearly planar (the angle between the least-squares planes of the pyridine substituents and of the napthyridine has an average value of 5.4°). The equatorial Rh(1)–N(2) and Rh(2)–N(3) bond lengths (average value 2.00 Å) are significantly shorter than the axial Rh(1)–N(1) and Rh(2)–N(4) distances (2.20 Å). The latter distances are just slightly shorter than the axial Rh–N distances in VI. The constraint of attaching the pyridyl ligand to the naphthyridine ring is evidenced in the Rh–Rh–N(axial) bond angles of 166.9 ± 0.1 and 180.0° for I and VI, respectively.

NMR Spectra. The ^{1}H NMR spectrum of I in Me_2SO-d_6 suggests that the structure represented in Figure 1 is maintained in solution. In the aromatic region, the 500-MHz spectrum shows six resonances of equal intensity (Table IV) consistent with a symmetrical bridging mode for the 12-proton bpnp ligand. In the methyl region, two singlets at δ 1.38 and 2.21 in an intensity ratio of 2:1 represent the acetates coordinated cis and trans to the aromatic ligand, respectively. The upfield shifts of the cis acetate methyls relative to the trans methyl and those seen for $Rh_2(OAc)_4$ (Table V) can be attributed in large part to the effects of aromatic ring currents in the naphthyridine ligand.

Similar patterns can be seen for the acetate methyl proton resonances in the other two monosubstituted complexes $Rh_2(OAc)_3(dinp)^+$ and $Rh_2(OAc)_3(pynp)^+$. In both cases two methyl singlets were observed with the upfield singlet having an intensity double that of the other (Table V). Thus, a structure analogous to that of I with one naphthyridine derivative and three acetates bridging the dirhodium(II) unit is indicated. In contrast one methyl singlet is seen for $Rh_2(OAc)_2(pynp)_2^+$. The upfield position of this resonance (δ 1.76) would be consistent with a structure having both acetates and both pynp ligands bridging the dirhodium(II) unit. In the same context it is notable that the 500-MHz spectrum of IV shows nine resonances in the aromatic region (Table VI) corresponding to the nine protons of pynp, further indicating the equivalence on the NMR time scale of the two pynp ligands. Two of the aromatic resonances, i and h (see structures in Introduction), are shifted upfield 1.52 and 0.37 ppm, respectively, from the corresponding resonances of the monopynp complex III while none of the other proton signals shift more than 0.16 ppm.

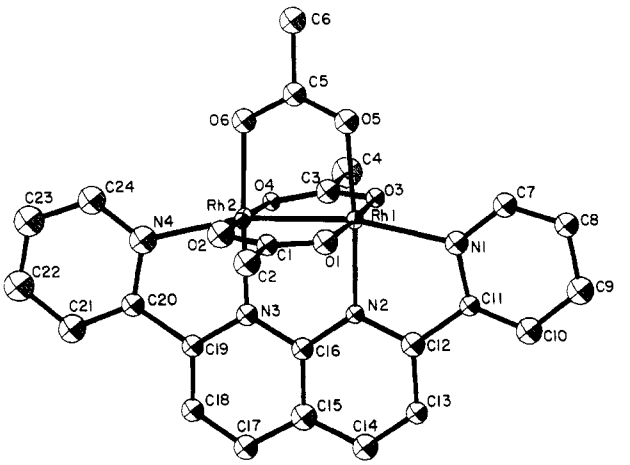

Figure 2. Perspective view of the tris(μ-acetato)(2,7-bis(2-pyridyl)-1,8-naphthyridine)dirhodium(II) cation. The hydrogen atoms have been omitted.

There are two structures for IV that could have the two pynp and the two acetate ligands in equivalent bridging positions: the C_{2h} trans configuration (A) and the C_2 cis configuration

(B). Molecular models suggest A to have the considerably greater steric crowding between the pynp ligands. Furthermore, these models show the i and h protons of each pynp for structure B to be positioned above the plane of the pyridyl fragment of the other pynp. Such a configuration (cis pynp ligands) would explain the anomalous upfield shifts of these two proton resonances for IV relative to III.

The proton NMR spectrum of V displays only three resonances of equal area at δ 9.94, 8.34, and 7.51 corresponding to the a, c, and b protons of np. This indicates that the four np ligands are equivalent on the NMR time scale. Structurally equivalent np's would be the case for the tetrakis(μ-1,8-naphthyridine) configuration or one in which the two rhodium(II) centers are each chelated by two 1,8-naphthyridines and joined by a single rhodium–rhodium bond. The former

Table VI. ^{1}H NMR Data for the Aromatic Regions of Naphthyridine-Substituted Dirhodium(II) Acetates II, III, and IV (Conditions as in Table III)

$Rh_2(OAc)_3(dinp)^+$			$Rh_2(OAc)_3(pynp)^+$			$Rh_2(OAc)_2(pynp)_2^{2+}$		
H	δ	J, Hz	H	δ	J, Hz	H	δ	J, Hz
a	9.42	ab, 4.2; ac, 1.6	a	9.59	ab, 5.9	a	9.70	ab, 4.8
b	7.98	ba, 4.0; bc, 8.3	b	8.24	ba, 5.9; bc, 8.0	b	8.40	ab, 4.8; bc, 7.7
c	8.73	cb, 8.3; ca, 1.6	c	8.60	cd, cb, 8.4; ca, 2.1	c	8.72	ca, 1.6; cb, cd, 8.4
d	8.68		d	9.09	cd, 7.7	d	9.21	cd, 7.9
e	8.96		e	8.88	ef, 8.8	e	8.84	ef, 8.9
f	8.76	fg, 8.3; fh, 2.0	f	9.04	ef, 8.8	f	9.09	fe, 8.9
g	8.01	gf, 8.4; gh, 5.4	g	8.78	gh, 8.0; gi, 2.2	g	8.64	gh, 8.4; gi, 1.6
h	10.14	hg, 5.4; hf, 2.0	h	8.00	hg, 8.0; hi, 5.4	h	7.63	hi, 5.5; hg, 8.4
			i	10.14	ih, 5.1; ig, 2.3	i	8.62	ih, 5.8

Table VII. Electronic Spectra of Dirhodium(II) Complexes Having Bridging Naphthyridine-Type Ligands (in Acetonitrile Solution)

complex	λ_{max}[a] (log ϵ)
$[Rh_2(OAc)_3(bpnp)]PF_6 \cdot 2H_2O$	578 (3.52), 540 sh (3.40), 440 sh (3.08), 408 sh (3.34), 363 (4.63), 346 (4.46), 283 (4.33), 248 (4.69)
$[Rh_2(OAc)_3(dinp)]PF_6 \cdot 3H_2O$	565 (3.51), 394 (4.30), 363 (4.34), 230 (4.67)
$[Rh_2(OAc)_3(pynp)]PF_6$	517 (3.56), 328 (4.45), 248 (4.49), 220 (4.56)
$[Rh_2(OAc)_2(pynp)_2](PF_6)_2$	472 (3.70), 356 (4.38), 320 (4.55), 278 (4.62), 249 (4.63)
$[Rh_2(np)_4]Cl_4 \cdot 4H_2O$	480 (2.18), 362 (4.21), 293 (4.42), 264 (4.66)
$Rh_2(OAc)_4(CH_3CN)_2$[b]	552 (2.37), 437 (2.10)
$Rh_2(OAc)_4(py)_2$[b,c]	518 (2.32)

[a] In nm; spectra obtained at ambient temperature. [b] Johnson, S. A.; Hunt, H. R.; Newmann, H. M. *Inorg. Chem.* **1963**, *2*, 960. [c] In neat pyridine.

structure has analogues in other tetrakis(μ-1,8-naphthyridine) complexes[10,11] including the structurally characterized $[Ni_2(np)_4]Br_3$, which has a Ni–Ni bond length of 2.415 Å, close to the 2.405-Å Rh–Rh distance seen in I.[12] The latter structure has an analogue in the tetrakis(dimethylglyoxime)dirhodium(II) complex characterized previously by Cotton.[13] Our current data do not differentiate between these two possibilities although observation of bridging 1,8-naphthyridines in other systems described in this manuscript leads us to favor the former configuration.

Electronic Spectra. Table VII summarizes the visible-region spectra of compounds I–V. In acetonitrile the naphthyridine-substituted dirhodium(II) complexes display intense ($\epsilon > 10^3$ M^{-1} cm^{-1}) low-energy absorption bands. These are generally solvent dependent. For example, the λ_{max} for the longest wavelength band of I occurs at 590, 578, and 569 nm, respectively, for solutions in tetrahydrofuran, acetonitrile, and methanol. Although bands of similar energy are also apparent in the visible spectra of $Rh_2(OAc)_4L_2$ (L = CH_3CN, pyridine, etc.) (Table VI), the intensities of these are more than an order of magnitude smaller. Earlier workers[1,15] have assigned the configuration of the Rh_2^{4+} core electrons as $\sigma^2\pi^4\delta^2\pi^{*4}\delta^{*2}$ and the lowest energy electronic transitions as $\delta^* \rightarrow \sigma^*$ and $\pi^* \rightarrow \sigma^*$.[16] The much greater intensities of the visible-range bands of I–IV might be attributable to the decreased symmetry of these complexes (relative to $Rh(OAc)_4L_2$) raising the transition moment integrals of the $\delta \rightarrow \sigma^*$ bands. However, a more likely assignment would be as metal to ligand charge transfers (MLCT). For example, in the C_{2v} symmetry of the $Rh_2(OAc)_3(bpnp)^+$ ion there are several allowed transitions from the highest occupied orbitals of the Rh_2^{4+} core to the lowest unoccupied π orbitals of the naphthyridine chromophore. Such MLCT bands are ubiquitous to the polypyridine complexes of low-valent metals.

Electrochemistry. Table VIII summarizes the oxidation and reduction potentials as determined by cyclic voltammetry in acetonitrile for the various dirhodium(II) complexes reported here. Compounds I–IV each undergo reversible one-electron oxidations and one or more reversible reductions. For solubility purposes the cyclic voltammetry of $[Rh_2(np)_4](PF_6)_4$ was carried out in dimethylformamide solvent, but no oxidative wave was seen for potentials below +1.5 V (vs. SSCE), and the only reduction was an irreversible wave at −1.6 V. In comparison the cyclic voltammetry of $Rh_2(OAc)_4$ in acetonitrile solvent displayed a single reversible oxidation at +1.02 V but irreversible reduction at −1.08 V.

Table VIII. Reduction and Oxidation Potentials for Naphthyridine Complexes of Dirhodium Acetate in CH_3CN (0.1 M TBAP) at 25 °C

	$E_{1/2}$, V (vs. SSCE)		
complex	oxidn	redn 1	redn 2
$Rh_2(OAc)_4$	1.02	−1.08[a]	
$Rh_2(OAc)_3(bpnp)^+$	1.28	−0.57	−1.21
$Rh_2(OAc)_3(dinp)^+$	1.34	−0.61	−1.10
$Rh_2(OAc)_3(pynp)^+$	1.26	−0.72	
$Rh_2(OAc)_2(pynp)_2^{2+}$	1.15	−0.60, −0.74	−1.34, −1.54
free bpnp		−1.56	

[a] Irreversible reduction.

The data in Table VIII indicate that replacement of one acetate by a naphthyridine tends to make the oxidation potential more positive relative to that seen for $Rh_2(OAc)_4$ (actually $Rh_2(OAc)_4(CH_3CN)_2$ in the CH_3CN solvent). The $E_{1/2}$ values for oxidation have been recorded for several $Rh_2(RCO_2)_4L_2$ complexes in different solvents (where L = solvent) with the general result being that potentials are several tenths of a volt smaller when L is the good donor pyridine than when L is acetonitrile.[17] Thus, for the $Rh_2(OAc)_3(bpnp)^+$ ion, where the two axial sites are occupied by the pyridyl substituents, the +1.28 V $E_{1/2}$ for oxidations vs. +1.02 V for $Rh_2(OAc)_4(CH_3CN)_2$ must be attributed to replacing one bridging acetate by the bridging naphthyridine fragment of bpnp. Earlier studies of the $Rh_2(RCO_2)_4L_2$ species have shown that electron-withdrawing R groups shift $E_{1/2}$(ox) to more positive potentials.[17] Thus, the bridging, uncharged naphthyridine functionality of complexes I–V may simply be less electron-donating than acetate, thus giving the less favorable oxidation potentials. A related argument would be that there is some back-bonding between the higher energy d orbitals of the dirhodium(II) core and the low-lying, unfilled π^* orbitals of the np chromophore, which have matching symmetries. A similar π-back-bonding argument was used to rationalize the oxidation $E_{1/2}$ values of the series of ruthenium(II) complexes $Ru(NH_3)_5L^{2+}$, where L is an aromatic nitrogen heterocycle.[18]

The observations of relatively facile, reversible reductions of complexes I–IV (Table VIII) lie in sharp contrast to those for the various $Rh_2(OAc)_4L_2$ complexes for which reduction occurs at more negative potentials and is irreversible.[17] Even more remarkable is the observation of the two reversible reductions for I and II and four for IV. This behavior resembles that of $Rh(bpy)_3^{3+}$ (bpy = 2,2′-bipyridine) for which multiple reversible reductions are observed.[19] In the latter case the reduction sites have been assigned to the aromatic ligands and a similar assignment would appear likely for complexes I–IV.

The very negative potential of the only reduction wave (irreversible) seen for V may suggest that in this case the lowest unoccupied orbital of the Rh_2^{4+} core (σ^* with respect to the metal–metal bond) may lie lower in energy than the π^* orbital of an unsubstituted np ligand. Such an ordering of these orbitals would be consistent with the electronic spectrum, which shows a low-intensity band ($\epsilon \approx 150$ M^{-1} cm^{-1}) at longer wavelengths than the broad, very intense absorption centered at 362 nm. By analogy to the other di-

(10) Balch, A. L.; Cooper, R. D. *J. Organomet. Chem.* **1979**, *169*, 97.
(11) (a) Schmidbaur, H.; Dash, K. C. *J. Am. Chem. Soc.* **1973**, *95*, 4855. (b) Dixon, K. R. *Inorg. Chem.* **1977**, *16*, 2618.
(12) Sacconi, L.; Mealli, C.; Gatteschi, D. *Inorg. Chem.* **1974**, *13*, 1985.
(13) Cotton, F. A.; Caulton, K. G. *J. Am. Chem. Soc.* **1971**, *93*, 1914.
(14) Sowa, T.; Kawamura, K.; Shida, T.; Yonezawa, T. *Inorg. Chem.* **1983**, *22*, 56.
(15) Norman, J.; Kolari, H. K. *J. Am. Chem. Soc.* **1978**, *100*, 791–799.
(16) Martin, D. S.; Webb, T. R.; Robbins, G. A.; Fanwich, P. E. *Inorg. Chem.* **1979**, *18*, 475.
(17) Das, K.; Kadish, K. M.; Bear, J. L. *Inorg. Chem.* **1978**, *17*, 930–934.
(18) Matsubara, T.; Ford, P. C. *Inorg. Chem.* **1976**, *15*, 1107.
(19) DeArmond, M. K.; Kew, G.; Hanck, K. *J. Phys. Chem.* **1974**, *78*, 727.

rhodium(II) spectra, these can be assigned as $\delta^*_{Rh_2} \rightarrow \sigma^*_{Rh_2}$ and MLCT transitions, respectively.

Summary. In this article we have outlined synthesis procedures for the replacement of bridging acetates of $Rh_2(OAc)_4$ by polydentate naphthyridine derivatives. The resulting complexes $Rh_2(OAc)_3L^+$, $Rh_2(OAc)_2L_2^{2+}$, and $Rh_2L_4^{4+}$ show intense absorption bands in the visible spectra, which have been tentatively assigned as metal to ligand charge-transfer bands. Several of these complexes display a very rich electrochemistry, undergoing both reversible oxidation and several reversible reductions as observed by cyclic voltammetry. The chemistry of these complexes, including potential catalyst applications, is under further investigation in these laboratories.

Acknowledgment. We acknowledge the U.S. Department of Energy (P.C.F.) and the Army Research Office, Durham (W.C.K.), for partial support. The 500-MHz NMR spectra were obtained with the help of Dr. Croasmun at the NSF Regional Facility, California Institute of Technology. We thank Alvaro Pardey of this department for some experimental assistance. We are grateful to Professor C. E. Strouse, Department of Chemistry, UCLA, for use of X-ray facilities and for valuable advice in the crystal structure determination.

Registry No. I, 88156-57-4; II, 88156-59-6; III, 88156-61-0; IV, 88156-63-2; V, 88156-64-3; Rh, 7440-16-6.

Supplementary Material Available: Tables IX (hydrogen atom positional and thermal parameters), X (anisotropic and isotropic thermal parameters for non-hydrogen atoms), XI (interatomic distances and angles of bpnp in I), and XII (observed and calculated structure factors) (15 pages). Ordering information is given on any current masthead page.

Contribution from Research Institute for Materials, Faculty of Science, Toernooiveld, 6525 ED Nijmegen, The Netherlands

Intermediates in the Formation of Gold Clusters. Preparation and X-ray Analysis of $[Au_7(PPh_3)_7]^+$ † and Synthesis and Characterization of $[Au_8(PPh_3)_6I]PF_6$

J. W. A. VAN DER VELDEN,* P. T. BEURSKENS, J. J. BOUR, W. P. BOSMAN, J. H. NOORDIK, M. KOLENBRANDER, and J. A. K. M. BUSKES

Received February 3, 1983

The evaporation of metallic gold into a toluene solution containing PPh_3 (L) leads to the formation of a number of compounds from which the heptanuclear $[Au_7L_7]^+$ ($C_{126}H_{105}Au_7P_7^+$) can be isolated as the major constituent. An X-ray analysis has been performed on a single crystal, space group $P\bar{1}$, with cell dimensions a = 34.94 (1) Å, b = 44.25 (2) Å, c = 15.45 (1) Å, α = 99.98 (3)°, β = 102.66 (3)°, γ = 88.11 (3)°, V = 22 953.5 Å^3, and Z = 8. The final R value is 0.099. The gold atoms in the $[Au_7L_7]^+$ cation form a slightly distorted pentagonal bipyramid, which is a novel feature for heptanuclear metal clusters. The axial Au–Au distance (average 2.584 ± 0.001 Å) is the shortest distance ever found in gold clusters. The axial–equatorial and equatorial–equatorial Au–Au distances have mean values of 2.82 ± 0.08 and 2.95 ± 0.06 Å, respectively. All P–Au vectors point approximately to the center of the cluster with normal P–Au distances (2.27 ± 0.09 Å). Physical data including ^{197}Au Mössbauer and (solid-state) $^{31}P\{^1H\}$ NMR are reported. $[Au_7L_7]^+$ can also be observed during the reaction of L with the novel compound $[Au_8L_6I]PF_6$. The latter cluster could be prepared from the reaction of $[Au_9L_8]^{3+}$ with Bu_4NI. The intermediacy of the title compounds in the formation and reactivity of gold cluster compounds will be discussed.

Introduction

The synthesis and the reactivity of gold phosphine clusters have been thoroughly studied during the last few years.[1] The fast formation of gold clusters containing 9 or 11 gold atoms by the reduction of Au(I) compounds can be observed under mild conditions, e.g., with ethanolic sodium borohydride as reducing agent at room temperature. Conversion reactions can occur for cationic gold phosphine clusters with Lewis bases, leading to other gold clusters within minutes. In particular, the reactions of $[Au_9L_8]^{3+}$ (L = PPh_3) have been studied intensively, showing that it can function as a starting material for the synthesis of gold clusters ranging in size from 4 to 11 gold atoms.[1] The presence of small intermediates, containing 2–4 Au atoms, has been suggested during both the formation and the conversion reactions of these compounds.

As the metal evaporation technique has proven to be a successful method for the synthesis of gold clusters in good yield,[2] we tried to isolate such a small intermediate from the reaction of gaseous gold atoms with L in toluene. This attempt was not successful, but led, however, to the discovery of a novel gold cluster compound, the heptanuclear $[Au_7L_7]^+$. $^{31}P\{^1H\}$ NMR experiments show that it is also formed quantitatively in the reaction of excess L with $[Au_8L_6I]PF_6$, which is a novel product obtained from the reaction of $[Au_9L_8]^{3+}$ with Bu_4NI. The bruto formula and the structure of the Au_7 cluster were found by X-ray analysis. Physical data are provided from both novel compounds in this report.

Experimental Section

Measurements. Elemental analyses and molecular weight determinations were carried out in our microanalytical department and by Dr. A. Bernhardt, Elbach über Engelskirchen, West Germany. $^{31}P\{^1H\}$ NMR spectra were recorded on a Varian XL-100 FT (solution; ^{31}P, 40.5 MHz) or a home-built NMR instrument[3] (solid state; ^{31}P, 72.9 MHz), IR spectra on a Perkin-Elmer 283, ESR spectra on a Varian E12, and ^{197}Au Mössbauer spectra with the apparatus described earlier.[4] All solvents were of reagent grade and used without further purification.

† The identity of the anion is uncertain.

(1) Steggerda, J. J.; Bour, J. J.; van der Velden, J. W. A. *Recl. Trav. Chim. Pays-Bas* **1982**, *101*, 164.
(2) Vollenbroek, F. A.; Bouten, P. C. P.; Trooster, J. M.; van den Berg, J. P.; Bour, J. J. *Inorg. Chem.* **1978**, *17*, 1345.
(3) Veeman, W. S.; Menger, E. M.; Ritchey, W.; de Boer, E. *Macromolecules* **1979**, *12*, 924.
(4) Viegers, M. P. A.; Trooster, J. M. *Phys. Rev. B: Solid State* **1977**, *15*, 72.

0020-1669/84/1323-0146$01.50/0